# MetA is a 'thermal fuse' that arrests growth and protects *Escherichia coli* at elevated temperatures

Severin Schink[1,2,#,*], Zara Gough[2,#], Elena Biselli[2,#], Mariel Garcia Huiman[2], Yu-Fang Chang[1], Markus Basan[1], Ulrich Gerland[2,*]

[1] Department of Systems Biology, Harvard Medical School, 200 Longwood Ave, 02115 Boston, MA, USA

[2] Physics of Complex Biosystems, Physics Department, Technical University of Munich, 85748 Garching, Germany

[#]Contributed equally

*Corresponding authors: severin_schink@hms.harvard.edu and gerland@tum.de

**Abstract**

Adaptive stress resistance in microbes is mostly attributed to the expression of stress response genes, such as heat shock proteins, which prevent deterioration of cellular material. Here, we report a novel response of *E. coli* to heat stress: induction of a growth-arrested state, caused by degradation of an enzyme in the methionine biosynthesis pathway (MetA). While MetA degradation is detrimental for proliferation, we show that the resulting growth arrest has a direct benefit for survival at high temperatures; it protects cells when temperatures rise beyond 50°C, increasing the survival chances by over 1000-fold. Using a combination of experiments and mathematical modelling, we show that degradation of MetA leads to the coexistence of growing and non-growing cells, allowing microbes to bet-hedge between continued growth if conditions remain bearable and survival if conditions worsen. We test our model experimentally and verify quantitatively how protein expression, degradation rates and environmental stresses affect the partitioning between growing and non-growing cells. Because growth arrest can be abolished with simple mutations, such as point mutations of MetA and knock-outs of proteases, we interpret the breakdown of methionine synthesis as a system that has evolved to disintegrate at high temperature and shut off growth, analogous to 'thermal fuses' used in engineering to shut off electricity when the device could be damaged by overheating.

34 **Introduction**

35 Microbes in nature face a variety of environments, ranging from ideal growth
36 conditions to hostile environments, where stressors threaten their survival. One
37 such stressor is elevated temperature, which can arise quickly and unpredictably.
38 When temperatures rise above the optimal range, microbes employ a well
39 characterized heat shock response [1–3]. Molecular chaperones protect proteins in
40 the cytoplasm and periplasm by maintaining their native conformation [4,1,2] and
41 proteases degrade misfolded and aggregated proteins [5]. DNA repair is
42 upregulated[6] and toxic reactive oxygen species, which are at particularly high
43 levels at elevated temperatures [7], are scavenged by catalases [8], superoxide
44 dismutases [9], and small molecules like glutathione [10,11]. The induction of these
45 protective genes, collectively referred to as the heat shock response, permits cells
46 to maintain their functionality and recover once conditions have improved.

47

48 However, some responses of microbes appear less logical. A long-standing puzzle
49 is the active degradation of a key enzyme in the methionine biosynthesis pathway,
50 homoserine O-succinyltransferase (MetA), when temperatures increase [12–14]. This
51 degradation causes methionine limitation, which slows the growth of cultures not
52 supplemented with methionine [12,15] and decreases the maximum growth
53 temperature in minimal medium from 47°C to 45°C [16]. The degradation of MetA
54 was found across bacterial species from Enterobacteriaceae, including *Escherichia*
55 *coli, Salmonella typhimurium* and *Klebsiella aerogenes*[17] to Alphaproteobacteria
56 like *Agrobacterium fabrum* [18]. Even in the gram-positive *Paenibacillus polymyxa*[19]
57 and *Corynebacterium glutamicum*[20], in which MetA and MetXA, respectively,
58 encode a homoserine o-acetyltransferase rather than a o-succinyltransferase, the

59 temperature-dependent degradation is conserved. This conservation is
60 conspicuous because MetA is only weakly conserved between these species (Fig.
61 S1), but is the only biosynthetic enzyme which is degraded at high rates [15].
62 Furthermore, MetA degradation is not inevitable, since several point-mutations
63 were discovered that decrease degradation rates, alleviate growth defects and
64 increase the maximum growth temperature [16,21]. Ron and coworkers
65 hypothesized that MetA could serve as a regulatory protein [14,15,17], given that it
66 displays rapid ATP-dependent proteolysis in combination with activation of
67 transcription [13,14], a hallmark of regulatory proteins that enable quick response
68 times [22]. However, it is unclear why stalling methionine biosynthesis should be
69 actively regulated by bacteria, because there would need to be "some undisclosed
70 selective benefit", as Ron and Davies put it [12]. To date, the only described benefit
71 is an increase in antibiotic persistence at elevated temperatures, discovered by
72 Mordukhova and Pan [23], but there is no apparent relation between antibiotic
73 stress and heat stress.
74
75 Here, we identify the missing selective benefit of MetA degradation. Furthermore,
76 we confirm the hypothesis that MetA dual-serves as a biosynthetic protein and a
77 temperature-sensitive regulatory protein, and clarify the mechanism whereby
78 MetA controls growth at elevated temperatures. Using *Escherichia coli* as a model
79 system, we show that MetA plays the central role in a new type of regulated
80 growth arrest that protects from cell death when temperature is further
81 increased. The protective effect of growth arrest against heat shocks appears to
82 be a more general physiological feature of microbes, as we can reproduce the
83 phenomenon in *Saccharomyces cerevisiae*. Hence, heat-induced growth arrest

84 appears to implement a `heat persistence' strategy that is conceptually similar to
85 antibiotic persistence [24]. While the regulatory mechanism controlling antibiotic
86 persistence remains elusive, we find that heat persistence is caused by a bistability
87 in growth that is modulated by MetA degradation.

88 **RESULTS**

89 *Elevated temperatures induce growth arrest in E. coli*

90 To probe how heat affects the physiology of bacteria, we exposed cultures of
91 *Escherichia coli* K-12 grown in minimal medium at elevated temperatures to a
92 period of carbon starvation. During this period, the absence of *de novo* synthesis
93 reveals the deteriorative effects of temperature on the cell. After the starvation
94 period, we reinoculated the culture in fresh medium with a carbon substrate and
95 observed the resulting recovery of the stressed culture. The temperature was kept
96 constant throughout the entire experiment, i.e. initial growth, starvation, and
97 recovery. We observed that the regrowth during the recovery phase displays lag
98 times that depend on temperature (Fig. 1A). At 37°C, cultures recovered quickly,
99 while at 45°C, the maximum growth temperature, the culture required more than
100 10 h to recover. Such long recovery times at high temperatures are puzzling,
101 because the majority of bacteria were still viable at the time of reinoculation, as
102 assayed by plating on LB agar at 37°C (Fig. S2), implying that the long lag times
103 are not due to cell death, but instead caused by viable bacteria not growing.

104

105 The lag time also increases with the prior starvation duration (Fig. 1B), suggesting
106 that cells gradually lose the ability to grow. For 1 hour of starvation, cultures
107 recovered within 2 hours, but if starvation took longer than 9 h at 45°C, cultures
108 did not recover within the 3 days of the experiment.

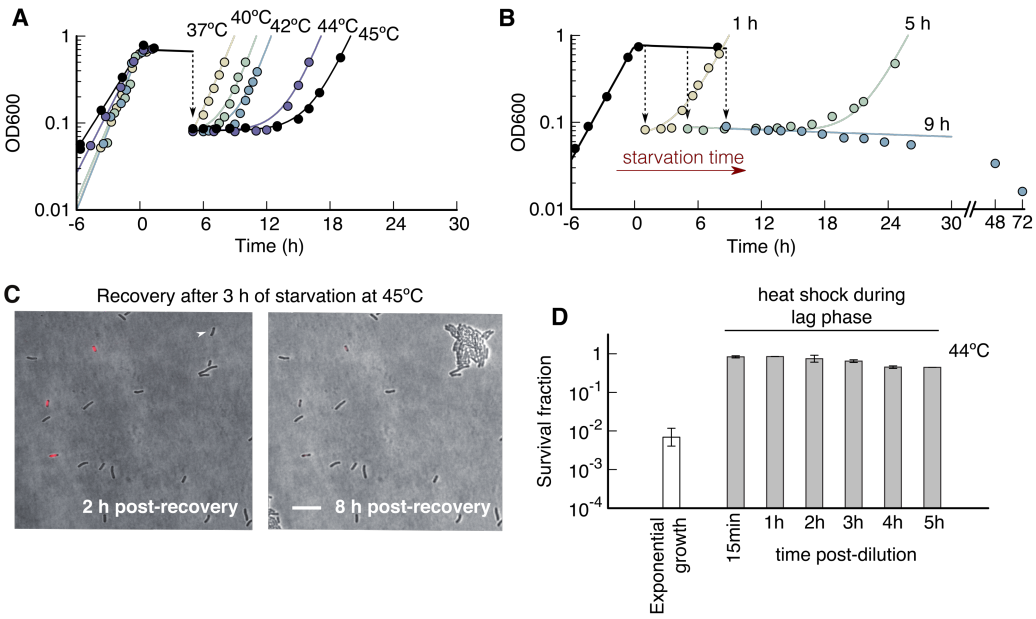


*Figure 1* ***Growth arrest at high temperatures protects Escherichia coli in heat shocks. (A)*** *Optical density $OD_{600}$ of Escherichia coli K-12 grown until nutrient depletion, first starved for 5 hours, then diluted into fresh medium to allow recovery. Colors denote culture temperatures, kept constant throughout each experiment. Lag times of cultures increase with temperature, from ~23 min at 37 °C, to 11.1 h at 45 °C. In panels A-C, growth is fitted as exponential $N(t) = N(0)e^{\mu t}$ and recovery as a combination of decay and growth $N(t) = N_1 e^{-\gamma t} + N_2 e^{\mu t}$, with $\gamma = 0.1\ h^{-1}$. Lag times are extracted as detailed in Methods.* ***(B)*** *Lag times at 45°C increase with starvation duration. No recovery was recorded within 3 days for 9 h starvation (blue) or longer.* ***(C)*** *Snapshots of time-lapse movies during recovery at 45 °C on glycerol minimal medium agar pads, see Methods. Fluorescence of propidium iodide (red) reports permeability. One growing cell (white arrow) grows to a microcolony after 8 h of incubation. Scale bar: 10 µm. (**D**) Killing by heat shock (52°C, 10min) of E. coli cultured at 44°C in exponential growth (white) or during lag phase after 3 h of starvation and dilution (grey). E. coli growth arrested during lag phase are completely protected from heat killing at 52°C.*

There are two qualitatively different scenarios for how long lag times can arise. One scenario is a homogeneous population of cells that all require a similarly long time to recover. The other scenario has two subpopulations, a large non-growing population and a small growing population. In the second case, the lag time is given by the time it takes for the small, growing population to dominate the cell count. To distinguish between these scenarios, we assayed the recovery phase at the single cell level: we extracted samples of a starved culture at 45°C and deposited them on pre-warmed agar pads supplemented with carbon substrate to

118 allow recovery. We stained the bacteria with propidium iodide (red) for
119 membrane permeability to detect cell death, and monitored growth by time-lapse
120 microscopy (see Methods). Figure 1C shows two snapshots from a time-lapse, 2 h
121 and 8 h after nutrient addition: The culture, previously starved for 3 h, shows
122 three distinct populations. 5% of the population stains positive for cell
123 permeability and are likely dead. A second, small subpopulation, 2%, recovered
124 after about 2 hours, and after 8 h has formed micro-colonies, which are visible in
125 Figure 1C (white arrow). The third and major subpopulation, 93%, stained
126 negative for cell permeability, but did not grow within the 12 h of this time lapse.
127 This data shows that recovery is highly heterogeneous; few cells recover early and
128 dominate the recovery.
129
130 In an experimental scenario similar to ours, Trip & Youk recently observed that
131 *Saccharomyces cerevisiae* arrest growth when cultures are diluted during
132 exponential growth at elevated temperatures[11]. Indeed, this density-dependent
133 growth behavior is shared by *E. coli*: we found that if cultures are diluted during
134 exponential growth, they also enter growth arrest (Fig. S5A). This poses an
135 interesting possibility that heat-induced growth arrest is a more general hallmark
136 of microbes, and triggers the question: Is there a fitness benefit to heat-induced
137 growth arrest ?
138
139 *Growth-arrest protects E. coli from heat shocks*
140 Because growth arrest is unique to temperatures close to the growth limit (40-
141 45°C for *E. coli)*, but in a regime where conditions still allow growth, we wondered
142 if growth arrest is an evolutionarily 'chosen' strategy, rather than an accident. For

143 such a strategy to evolve, there would need to be a selective benefit associated
144 with growth arrest, which outweighs the cost of reduced growth. To examine
145 possible selective benefits, we exposed *E. coli* cultures to sudden heat shocks. We
146 used our standard starvation protocol (Fig. 1A-C) to induce growth arrest, using a
147 5h period of starvation and subsequent reinoculation in fresh medium at 44°C. We
148 took samples from the culture every hour after reinoculation, heat shocked them
149 for 10 min at 52°C, and measured the resulting viability. Strikingly, growth-
150 arrested cultures survived heat shocks almost unscathed, while in cultures heat
151 shocked in exponential growth, only about 0.7% survived (Fig. 1D). The existence
152 of this benefit shows that growth arrest could in principle be used by
153 microorganisms as a part of the response to heat stress. To investigate this
154 possibilty, we next sought to understand what causes *E. coli* to enter growth
155 arrest.
156

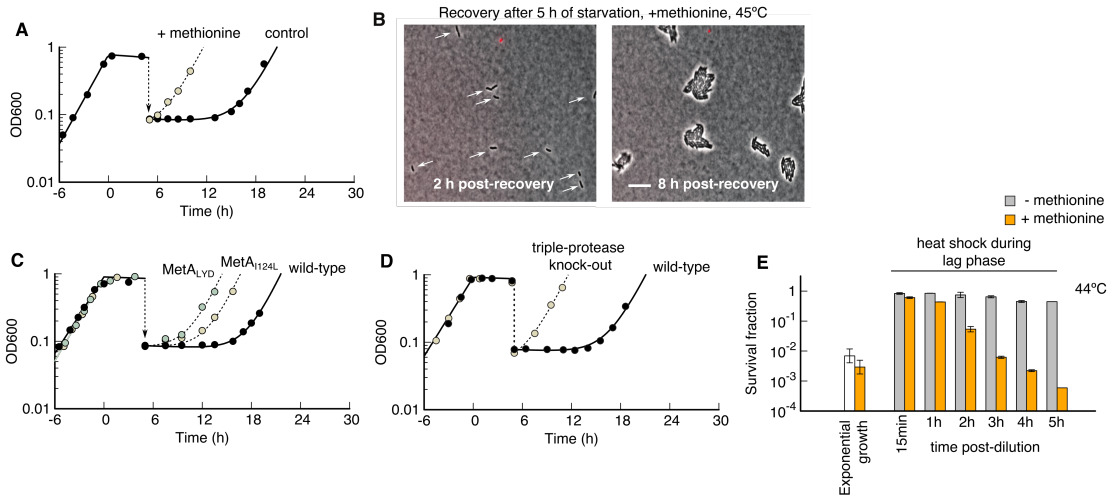


*Figure 2* ***Growth arrested cells are methionine limited due to MetA degradation. (A)*** *Cultures supplemented with methionine recover quickly. Lag times (45°C, 5 h starvation) in cultures supplemented with methionine during the entire experiment are more than 90% shorter than without methionine ($T_{lag} = (0.64 \pm 0.02)$ h compared to $T_{lag} = (11.08 \pm 0.4)$ h, N = 2, p < 0.001). (**B**) Snapshots of a time-lapse of recovery on glycerol agar pads supplemented with methionine. Cells indicated with white arrows recover and form microcolonies after 8 hours. Scale bar: 10µm. (**C**) Comparison of wild-type MetA with two thermostable mutants. Lag times (45°C, 5 h starvation) decrease in mutants MetA I124Y ($T_{lag} = (5.2 \pm 1.0)$ h, N = 3, p < 0.001) and LYD ($T_{lag} = (3.7 \pm 0.9)$ h, N = 3, p < 0.001) compared to wild-type ($T_{lag} = (11.1 \pm 0.3)$ h, N = 3). (**D**) Comparison of wild-type E. coli with a triple protease knock-out (Δlon, ΔhslV & ΔclpP). Absence of protease activity decreases lag time ($T_{lag} = (1.1 \pm 0.3)$ h, N = 3, p = 0.0012) compared to wild-type ($T_{lag} = (10.4 \pm 1.6)$ h, N = 3). (**E**) Heat shocks (10 min at 52°C) during exponential growth and during lag times at 44°C in cultures supplemented with and without methionine. Killing of the methionine-supplemented culture coincides with growth (at 2h: 2-fold increase of CFU/ml, at 5h: 20-fold increase of CFU/ml).*

*Breakdown of methionine synthesis causes growth arrest in E. coli*

It is known that high temperature leads to denaturation of the proteome [25,26]. One protein, homoserine O-succinyltransferase (MetA), which catalyzes the first commitment step of the methionine biosynthesis pathway, is particularly susceptible to heat stress [12–14]. This enzyme aggregates and is degraded [15]. To test if the long lag times are due to methionine limitation, we supplemented the medium with methionine and found a drastic reduction in lag time, from over 10 hours without methionine, down to less than 30 minutes with methionine (Fig. 2A). Similarly, growth arrest induced by dilution was also alleviated by the presence of methionine, decreasing the minimum initial population density from

167 which cultures could regrow 100-fold (Fig S5). Investigating lag times on a single-
168 cell level, we found that if the agar pad is supplemented with methionine, the
169 majority of the cells recovered after starvation (63% compared to 2% w/o
170 methionine), while the growth-arrested and non-permeable subpopulation
171 virtually disappeared (5% compared to 93% w/o methionine), see Figure 2B. The
172 absence of the growth-arrested subpopoulation (Fig. 2B) is consistent with the
173 drastic reduction in lag times observed in bulk measurements (Fig. 2A).
174
175 To test if methionine limitation is due to MetA degradation, and not a different
176 enzyme in the methionine pathway, we tested MetA mutants with reduced
177 degradation rates, either due to a single point mutation (I124L) or three point
178 mutations (I124L-I229Y-N267D – abbr. LYD) identified by Mordukhova and
179 coworkers [21]. Indeed, these mutants, which have 2-3 fold decreased degradation
180 rates [21], showed a significant decrease in lag times from about 11 h to about 5 h
181 for the single point mutant (I124L) and 4 h for the triple-point mutant (LYD) (Fig.
182 2C).
183
184 When we hypothesize growth arrest to be a response to heat stress, an important
185 question is whether MetA is degraded because it is broken, e.g. aggregated or
186 otherwise damaged, or whether MetA is degraded despite being still functional.
187 The latter option would speak for growth arrest being a 'self-inflicted injury',
188 rather than an accident. To distinguish these two possibilities, we constructed a
189 triple knock-out of proteases Δ*lon, ΔhslV* and Δ*clpP,* incapable of degrading
190 cytoplasmic proteins, in particular MetA[14]. If MetA is broken, lag times should
191 either remain unchanged or increase in this triple protease knock-out mutant. On

192 the other hand, if functional MetA is actively degraded in wild-type, lag times will
193 decrease in the mutant. In the experiment, we found a striking decrease of lag time
194 from 10 h in wild-type down to 1 h in the triple protease knock-out (Fig. 2D),
195 strongly suggesting that methionine limitation is caused by degradation of
196 *functional* MetA. This implies that the methionine limitation is brought upon the
197 cell by itself, rather than being caused exclusively by stressors.
198
199 If growth arrest protects *E. coli* during heat shocks, and growth arrest is in turn
200 due to methionine limitation, then the addition of methionine should render cells
201 susceptible to heat again. We tested this hypothesis on cultures that were grown,
202 starved, and reinoculated at 44˚C in media with and without methionine, and then
203 heat-shocked at 52˚C (see `Methods'). While cultures without methionine were
204 protected for several hours from heat, cultures with methionine lost more than
205 99.9% of their viability soon after reinoculation in fresh medium (Fig. 2E).
206
207 *Metabolic bistability leads to stable growth arrest*
208 How does methionine limitation trap cells in a state of growth arrest? This is
209 particularly important in order to understand which mechanisms microbes could
210 use to manipulate the fraction of cells entering growth arrest depending on
211 external conditions. While it is clear that degradation of MetA is detrimental for
212 growth, it is important to note how stable growth arrest is: entire cultures can
213 remain growth-arrested for several days, although the conditions would allow for
214 growth in principle (Fig. 1). This stability of growth arrest is puzzling because one
215 would expect that any residual amount of MetA activity, or import of methionine
216 from perished cells, would kickstart growth by supplying methionine, which in

217 turn will be used to synthesize MetA in a self-enhancing positive feedback loop. To
218 answer these questions, we designed a mathematical model of metabolism and
219 protein synthesis that describes the dynamics of internal methionine
220 concentration $c_{\mathrm{met}}$ and MetA abundance $\phi_{\mathrm{MetA}}$. We will use the model to derive a
221 theoretical prediction of lag time, and to perform quantitative tests of our
222 hypotheses.
223
224 The model, summarized in Fig. 3A, incorporates processes that affect the cellular
225 methionine level (solid lines) and the MetA protein abundance (dashed lines).
226 Within this model, growth is limited by methionine, Eq. (1), and MetA is degraded
227 at rate $\gamma$, diluted by growth and synthesized together with biomass at rate $\mu$, Eq.
228 (2). Methionine can either be produced by MetA, or taken up from the
229 environment, and is used for protein synthesis and to synthesize S-adenosyl-
230 methionine (SAM), the major methyl donor of the cell, Eq. (3). While much of this
231 SAM is recycled back to methionine in the SAM cycle (Fig. S3), a significant part is
232 used for biosynthesis of polyamines (Table S2), such as spermine and spermidine,
233 which are important for survival in stress conditions [27–29]. We account for SAM
234 synthesis and other potential losses of methionine flux in a drainage flux (Fig. 3A).
235 In the Supplementary Information we show a detailed derivation of the model and
236 in Table S2 we estimate model parameters based on published measurements.

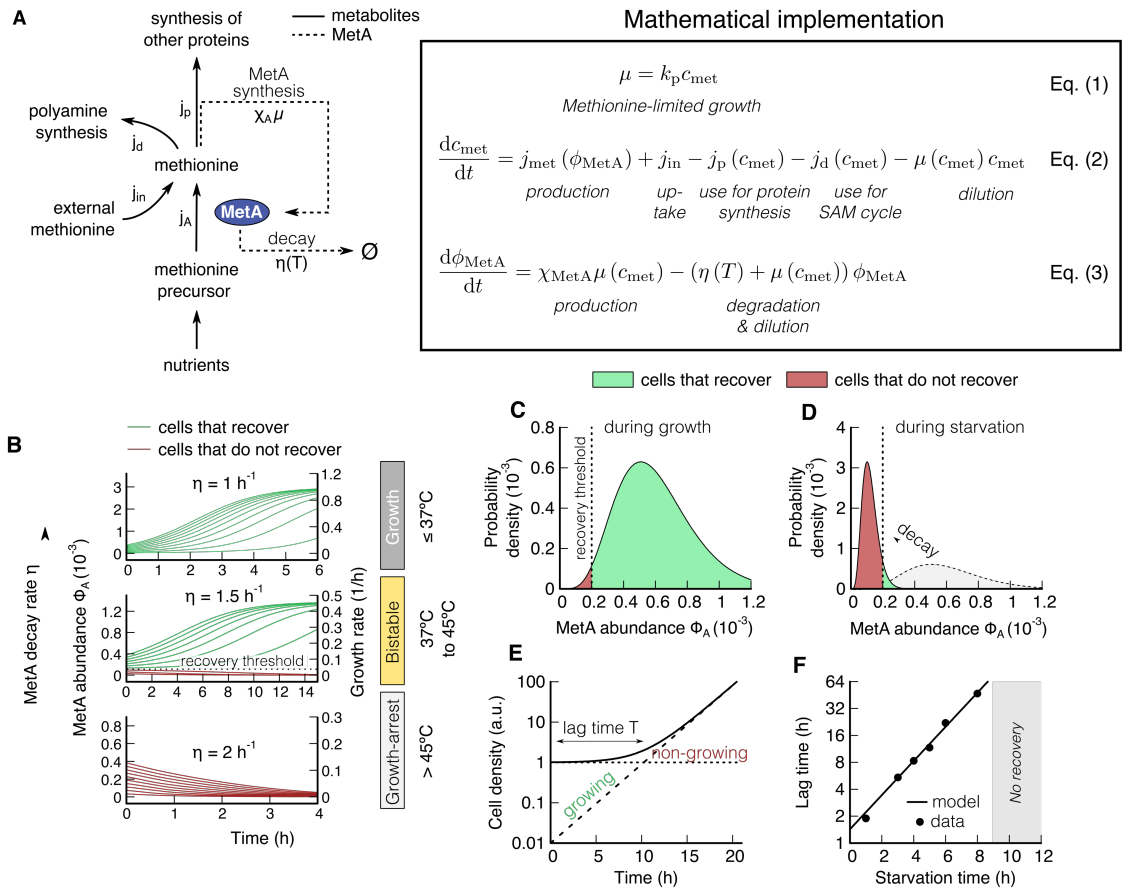


*Figure 3* ***Methionine-MetA model shows that bistability arises from dual use of methionine.*** *(**A**) Cartoon of the methionine-MetA model. Metabolites: nutrients are taken up, converted first to precursors and finally to methionine by MetA (pink). See Figure S3 for a detailed methionine biosynthesis pathway. External methionine can be imported, if present in the medium. Two fluxes drain methionine, protein synthesis and polyamine synthesis. Proteins: MetA (pink) is synthesized if methionine is present, and will in turn synthesize methionine (positive feedback loop). MetA is degraded at a temperature dependent rate.* ***(B)*** *Numerical results of the dynamics of the methionine-MetA model for three different MetA degradation rates (1.0/h, 1.5/h and 2/h). Whether cells can recover depends on the temperature dependent degradation rate. At intermediate temperatures (middle), we observe that only cells with an initial MetA abundance above a recovery threshold can recover (bistable regime).* ***(C-D)*** *Distribution of MetA abundance during growth and starvation. Green and red areas indicate cells with MetA abundance that allow (green) and do not allow (red) growth.* ***(E)*** *Recovery dynamics of a mixed culture in batch. The time it takes for the growing fraction to overgrow the non-growing fraction is the lag time.* ***(F)*** *Theoretical prediction of lag times compared with experiments (45°C). Lag time increases exponentially with starvation time* $T_{lag} = (1.6 \pm 0.3)\, exp(\tau\, (0.43 \pm 0.02)\, h^{-1})$*. When cultures are starved for more than 9 hours, they do not recover within three days. The exponential rate fitted,* $\eta = 0.46\, h^{-1}$*, is lower than the in-vitro MetA decay rate 1.6* $h^{-1}$ *measured in Ref. [27], possibly due to low levels of ATP that is required for active degradation during starvation [25].*

The recovery dynamics of the methionine-MetA model depends on the degradation rate of MetA (Fig. 3B): At low degradation rate, all cells, regardless of their initial state, recover to growth (top panel, green trajectories), while at high

241 degradation rate, none of the cells recover (bottom panel, red trajectories). In
242 between these two extremes, the population splits depending on the initial MetA
243 abundance (Fig. 3B, middle). Cells above a certain 'recovery threshold' accumulate
244 MetA and start growing, while cells below the threshold do not. Because both
245 growth and growth-arrest are stable states, this intermediate regime is bistable,
246 and a population can contain cells that are growing and others that are not.
247 Because of the positive-feedback motif between methionine and MetA, the
248 bistability requires a non-linearity in flux[30], which in our model is caused by the
249 drain of methionine to SAM and disappears if either the drain is shut off (Fig. S4A)
250 or if methionine is supplemented in the medium (Fig. S4B).
251
252 Because whether an individual cell recovers or stays dormant depends on its
253 initial MetA abundance, we suspect that fluctuations in MetA abundance cause the
254 split of the population. Protein abundance is indeed highly variable among
255 individual bacteria due to the stochasticity of transcription and translation
256 processes[31,32], with a typical standard deviation of 40% [32]. We thus hypothesize
257 that during growth, the vast majority of cells will lie above the recovery threshold
258 (Fig. 3C), and that only due to starvation at elevated temperatures, where MetA
259 will be degraded but not synthesized, the abundance distribution will shift to
260 lower values and many cells will fall below the threshold (Fig. 3D). As a result, only
261 the exponential tail of the MetA abundance distribution will remain above the
262 recovery threshold, leading to a small population of recovering cells. According to
263 the model, the characteristic long lag times observed in Fig. 1 emerge from this
264 mixture of growing and non-growing cells (Fig. 3E).
265

266 The model predicts (Supplementary Text 1C) how lag time depends on the
267 fraction of recovering cells, and how degradation of MetA reduces the fraction of
268 recovering cells. We find a simple exponential dependence between lag time $T_{\mathrm{lag}}$
269 and the starvation time $\tau$ and degradation rate $\eta$,

$$T_{\mathrm{lag}} \propto \bar{\phi}_{\mathrm{MetA}}^{-1} \exp(\eta\tau)\,, \qquad (1)$$

270 which originates from the exponential tail of MetA abundance, caused by the
271 stochasticity of transcription and translation processes ($\bar{\phi}_{\mathrm{MetA}}$ denotes the mean
272 MetA abundance).
273
274 A key prediction from the model in Eq. (4) is that the lag time $T_{\mathrm{lag}}$ should increase
275 exponentially with starvation time $\tau$. Because lag time in the model is set by the
276 fraction of the population that recovers, this dependence gives us a direct test of
277 what determines how many cells get trapped in the growth arrest state. Indeed,
278 we can verify the exponential scaling law, and find that it holds over a striking 50-
279 fold range in lag times (Fig. 3F). Cultures starved for more than 9 hours did not
280 recover within 3 days, presumably because all cells of the population are trapped
281 in the growth-arrested state.
282
283 The MetA mutants with reduced degradation rates give us the opportunity to test
284 how evolution can tune the fraction of growth-arrested cells, and hence the lag
285 time. The single point mutant I124L, has an experimentally measured degradation

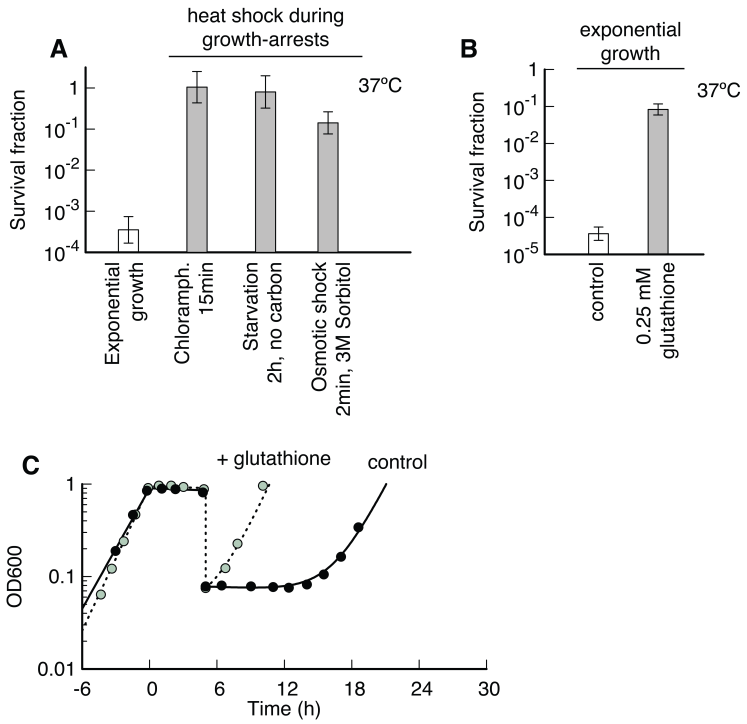


*Figure 4* ***Oxidative stress at elevated temperatures****. (**A**) Killing by heat shock (50°C, 10min) of E. coli cultured at 37°C either in exponential growth (white) or in growth arrest caused by translation inhibition (chloramphenicol), carbon starvation or hyperosmotic shock (grey). Protection from heat killing is independent of the cause of growth arrest. (**B**) Addition of the antioxidant glutathione rescues heat-induced death (50°C, 10 min) in exponential growth indicating that oxidative damage is involved at heat-induced death. (**C**) Addition of glutathione reduces lag times after 5h of starvation from ($T_{lag} = (1.4 \pm 0.2)$ h to $T_{lag} = (10.3 \pm 1.6)$ h, N = 3, p = 0.0013).*

rate reduced by 48% compared to wild-type[21]. Using the fit from Fig. 3F, we predict that this mutant should display a lag time of $T_{\mathrm{lag}} = (4.5 \pm 1.0)$ h, which matches the observed (5.2 $\pm$ 1.0) h of Fig. 2C well.

*Growth arrest protects cells irrespective of cause*

Finally, it is still unclear how heat-induced growth arrest protects cells from subsequent heat-shocks. One possibility is that heat shock proteins, expressed during growth arrest, prepare cells for the upcoming heat shock. To test this hypothesis, we blocked translation during exponential growth by adding chloramphenicol, which leads to growth arrest without new proteins being synthesized [33]. These experiments were performed at 37°C, where cells are particularly susceptible to subsequent heat shocks. Remarkably, cultures arrested

298 with chloramphenicol survived heat shocks without a significant decrease in
299 viability, whereas the viability of untreated cultures in exponential growth
300 decreased by more than 99.9% (Fig. 4A). Growth arrest by inhibition of protein
301 synthesis thus phenocopies the effect of methionine-limited growth arrest (Fig.
302 2E). Two alternative types of growth arrest, hyperosmotic shock (3M sorbitol) and
303 sudden carbon starvation (culture washed during exponential growth and
304 resuspended in carbon-free medium, then starved for 2 h, thus preventing
305 adaptation during the stationary phase), also yielded similar protection from heat
306 shocks (Fig. 4A), suggesting that growth arrest by itself, independent of the
307 underlying cause, is protective.
308
309 *Oxidative damage contributes to heat-induced death*
310 What are growth-arrested bacteria protected from? For eukaryotic microbes like
311 *Saccharomyces cerevisiae* [34,35] and animals like gold fish [36,37] it was shown that
312 oxidative damage is involved in heat-induced stress and death. To reduce
313 oxidative damage at high temperatures, *S. cerevisiae* exports antioxidants such as
314 glutathionine [11]. For bacteria, a similar connection between oxidative stress and
315 temperature stress was hypothesized, based on the observation that temperature
316 sensitive mutants are hypersensitive to oxidative stress [38]. To test if oxidative
317 stress is indeed involved in heat-induced death, we supplemented cultures in
318 exponential growth at 37°C with glutathione and performed heat shocks.
319 Strikingly, we found that glutathione-supplemented cultures in exponential
320 growth survive 1000-fold better compared to an untreated control (Fig. 4B). This
321 result indicates that growth arrest alleviates lethal oxidative damage that would
322 otherwise kill in heat shocks.

323

324 Because oxidative damage is well known to induce aggregation[39,40] and
325 proteolysis [41,42], akin to the aggregation and degradation observed for MetA at
326 high temperatures [14,15], we tested if adding the antioxidant glutathione in our
327 standard starvation and reinoculation protocol influences lag times. We found a
328 drastic reduction in lag times for cultures supplemented with glutathione, from
329 10.4 h to 1.4 h (Fig. 4C). Because lag times are caused by degradation of MetA (Fig.
330 2), this result suggests that oxidative damage is the trigger for MetA degradation.
331 Similarly, glutathione prevents growth arrest at elevated temperatures in yeast [11],
332 suggesting that oxidative damage causes growth arrest more generally in
333 microbes. To test if growth arrest in yeast is also caused by methionine limitation
334 or by a different mechanism, we tested if growth arrest of *Sacharomyces cerevisiae*
335 at 39°C can be rescued with methionine. We found no difference in growth
336 between methionine-supplemented cultures and controls (Fig. S6 A-B), showing
337 that for yeast, growth arrest is caused by a different mechanism. The protective
338 feature of growth arrest, however, is shared by yeast: While growing yeast (30°C)
339 died by a factor of 500 during heat shocks, starving yeast largly survived (Fig S6
340 C). Taken together, these findings show that employing growth arrest to combat
341 heat-induced death may be a more general strategy of microbes.

342 **DISCUSSION**

343 We have shown that breakdown of methionine biosynthesis at elevated
344 temperatures causes growth arrest in *Escherichia coli*. Despite its fitness cost
345 under habitable conditions, growth arrest is beneficial for *E. coli* because it
346 protects cells from heat-induced death when temperatures rise beyond 50°C. We
347 demonstrated that this growth arrest can be alleviated by simple point mutations
348 and knock-outs. We therefore suggest that it constitutes a self-controlled growth
349 arrest that has likely evolved as an active response to heat stress, orthogonal to
350 the well-studied heat shock response.

351

352 *Relation to 'viable but not culturable' (VBNC) and persistence states*

353 Growth arrest similar to the phenomenon described in our work is frequently
354 encountered in a variety of microbes across the phylogenetic spectrum [43] when
355 exposed to stress conditions outside of the optimal culture conditions [44,45,43]. A
356 growing body of literature suggests the importance of growth arrest in the context
357 of 'viable but not culturable' (VBNC) states[43,45] and persistence[24,46], in particular
358 in food safety[47,48] and antibiotic treatment[24]. However, pinning down mechanisms
359 of how bacteria achieve growth arrest and why such mechanisms have evolved
360 has proven challenging [49,50]. Our results show that proteolytic regulation of basic
361 biosynthetic pathways is an efficient strategy to robustly induce growth-arrest.

362

363 *Shut-off of methionine synthesis is ideally suited to halt growth*

364 While a lack of any amino acid would stop translation, lack of methionine
365 specifically halts translation initiation, because the majority of bacterial start
366 codons code for N-formylmethionine (fMet), a direct derivative of methionine.

367 Lack of other amino acids would halt elongation after initiation, leading to protein
368 fragments that would need to be recycled by the cell. Furthermore, inhibition of
369 translation triggers the stringent response alarmone (p)ppGpp [51]. This global
370 regulator in bacteria inhibits synthesis of rRNA and tRNA [52], transcription [53], as
371 well as DNA replication [54,55], leading to a global shut-off in macromolecule
372 synthesis. At the same time, the central metabolism and generation of energy-rich
373 molecules are upstream of MetA, so that cells are presumably well fueled to
374 perform energy-dependent maintenance. This combination of inhibited
375 biosynthesis, but non-inhibited metabolism makes methionine an ideal bottleneck
376 to induce growth-arrest in bacteria, which lack global regulators of growth, and
377 we therefore speculate that this is the reason the for conservation of temperature-
378 dependent methionine synthesis breakdown in bacteria across the phylogenetic
379 spectrum [17,19,20,18].
380
381 *MetA is a biological 'thermal fuse'*
382 The temperature-induced degradation of MetA has a counterpart in electrical
383 engineering: electrical devices are protected from excessive heat with 'thermal
384 fuses', which cut off electric current by physically disintegrating, typically by
385 melting. The fuse has the role of an emergency protection, kicking in when other
386 regulatory mechanisms have failed, in order to protect expensive components. In
387 this analogy, first suggested by Price-Carter et al [56] for acid stress, we interpret
388 MetA as a biological thermal fuse. If the benefit of increasing survival chances
389 outweighs the cost of increased synthesis and missed potential for growth, then
390 the thermal fuse will have a net positive effect on fitness. The high expression
391 levels combined with high degradation rates, as in the case of MetA, reflects a

highly volatile strategy, typical for biological regulators [22]. In fact, it is ideally suited to stressful conditions to ensure fast growth if conditions are bearable, while also quickly shutting off biosynthesis if conditions worsen.

*Bet-hedging between growth and survival in anticipation of rare catastrophic events*

The bistability in growth arrest could play a vital role in optimizing fitness at elevated temperatures. Because both growth and growth arrest are stable, the bacterial population can split into two subpopulations. If individual cells can switch between states of growth and arrest depending on the external environment and their internal methionine concentration, then according to the model, the fitness of the population is optimized by partitioning the population into two sub-populations; a growing and growth-arrested population. Such a mixture of two distinct behaviors in a genetically homogeneous population of cells is a hallmark of bet-hedging strategies, typical for biolgical systems in unpredictable environments [57–59]. Bet-hedging aims to increase long-term fitness beyond what would be possible for either pure strategies of growth and growth arrest. Thus having a growth-arrested subpopulation will allow microbes to survive sudden heat shocks, while at the same time proliferating at sub-critical temperatures – enabling them to robustly thrive at the edge of habitable conditions.

**Acknowledgments**

This work was supported by the German Research Foundation (DFG) via the Excellence Cluster ORIGINS (through U.G.), and by the Life initiative of the

Volkswagen Foundation (through U.G.). E.B. was supported by a DFG fellowship through the Graduate School of Quantitative Biosciences Munich (QBM). S.J.S was supported by a Long-Term Fellowship (ALTF 782-2017) from the European Molecular Biology Organization (EMBO) and Long-Term Fellowship (LT000597/2018-L) from the Human Frontiers in Science Program (HFSP).

**Author contributions**

SJS and UG conceived this study. SJS, EB, MGH and ZG designed and performed experiments. YFC constructed strains. SJS, MB and UG developd the theoretical model. SJS, EB, MB and UG wrote the paper. MB and UG funded and supervised the project.

**Data availability statement**

Source data of figures are available upon request from the corresponding authors.

**Code availability**

The numerical implementation of the theoretical model used to generate Figure 3 is available upon request from the coresponding authors.

**Declaration of interests**

The authors declare no competing financial interests.

438 **METHODS**

439 *Contact for Reagent and Resource Sharing*

440 Further information and requests for resources and reagents should be directed
441 to and will be fulfilled by the lead contact.

442

443 *Strains*

444 All strains used in this study are derived from wild type *E. coli* K-12 strain
445 NCM3722 [60]. Amino acid substitutions $MetA_{I229Y}$ and $MetA_{LYD}$ (containing point
446 mutations I124L-I229Y-N267D) in strains I229Y and LYD [21] were transferred to
447 NCM3722 ΔMetA via P1 transduction to yield strains YCE55 (NCM3722 $metA_{I229Y}$)
448 and YCE57 (NCM3722 $metA_{LYD}$), using methionine as a selective marker.

449

450 *Culture media*

451 The culture medium for *E. coli* used in this study is based on $N^-C^-$ minimal
452 medium [61], containing $K_2SO_4$ (1 g), $K_2HPO_4 \cdot 3H_2O$ (17.7 g), $KH_2PO_4$ (4.7 g),
453 $MgSO_4 \cdot 7H_2O$ (0.1 g) and NaCl (2.5 g) per liter. The medium was supplemented
454 with 20 mM $NH_4Cl$, as nitrogen source, and 5 to 10 mM glycerol, as the sole carbon
455 source. *S. cerevisiae* were cultured in yeast nitrogen base medium (without amino
456 acids) and supplemented with 0.5% glucose. All chemicals were purchased from
457 Carl Roth, Karlsruhe, Germany. When needed, 0.1 mg/ml ampicillin (stock
458 prepared fresh and stored at -20°C) and/or 0.067 mM methionine (stock stored
459 at 4°C) were added to the culture

460

461 *Growth protocol for E. coli*

462 Cells were taken from a -80°C glycerol stock, streaked out on a LB agar plate and
463 incubated around 12 hours at 37°C. A single colony was picked and grown in batch
464 culture. For temperatures up to 39°C, cells were grown first on LB at the desired
465 temperature (seed culture). Before reaching starvation, they were diluted and
466 inoculated into pre-warmed minimal medium supplemented with glycerol (pre-
467 culture). Cells grew in the pre-culture for several doublings to ensure exponential
468 growth and were then diluted and inoculated into pre-warmed glycerol minimal
469 medium (experimental culture). Inoculation into the latter was chosen such that
470 cells perform at least three additional doublings in the experimental culture
471 before growth was measured. For high temperatures (above 39°C), the seed
472 culture medium used was glycerol minimal medium with 1% LB in order to help
473 the cells transition into the pre-culture.
474
475 For small culture volumes, 5 ml of culture were grown in 20 mm × 150 mm glass
476 test tubes (Fisher Scientific, Hampton, NH, USA) with disposable, polypropylene
477 Kim-Kap closures (Kimble Chase, Vineland, NJ, USA). Larger volumes, 25 ml, 50 ml
478 and 100 ml were grown in 125 ml, 250 ml and 500 ml baffled Erlenmeyer flasks
479 (Carl Roth, Karlsruhe, Germany), respectively, and Kim-Kap closures. All cultures
480 were grown in a shaking water bath (WSB-30, Witeg, Wertheim, Germany) with
481 water bath preservative (Akasolv, Akadia, Mannheim, Germany).
482
483 *Growth protocol for S. cerevisiae*
484 Cells were streaked from a -80°C glycerol stock onto a YPD agar plate and
485 incubated for approximately 30 hours at 30°C. A single colony was picked and
486 grown in batch culture with 4 mL NBM containing 1% YPD. Where necessary, the

487 culture was supplemented with methionine (0.067 mM). All cultures were
488 incubated in a shaking water bath with the culture tubes angled parallel to the
489 direction of shaking. The culture tubes and shaking water bath used were identical
490 to those used for the cultivation of *E. coli*.
491
492 *Protocol to induce long lag times at high temperatures*
493 Bacteria were first grown in minimal medium supplemented with glycerol as a
494 carbon substrate, as described above, at the desired temperature (37 to 45°C).
495 After carbon depletion, cultures starved for 1 h to 24 h. Then, cultures were
496 diluted into fresh $N^-C^-$ supplemented with glycerol and $NH_4Cl$ and allowed to
497 recover.
498
499 *Quantification of lag time*
500 The lag time after glycerol re-addition was extracted from optical density
501 measurements, and corrected for the loss of viability during the period of
502 starvation. Growth was modeled as $\mathrm{OD}_{600} = A + Be^{\mu t}$, which for long times
503 converges to $\lim_{t\to\infty} \mathrm{OD}_{600} = Be^{\mu t} = (A+B)e^{\mu(t-T_{\mathrm{lag}})}$, with lag time $T_{\mathrm{lag}}$. We
504 extracted growth rate $\mu$ and the growing fraction of cells, $B$, from the time
505 derivative of optical density $\mathrm{d}\,\mathrm{OD}_{600}/\mathrm{d}t = \mu B e^{\mu t}$, using a least square fit across
506 the recovery regime where the time derivative increases exponentially. We
507 measure $(A+B)$ as the optical density after dilution. The lag time $T_{\mathrm{lag}} =$
508 $-\mu^{-1}\ln(B/(A+B))$, can then be calculated from the extracted parameters.
509 Lastly, because optical density measurements do not distinguish between living
510 and dead cells in the culture, and a fraction of the culture has perished during

511 starvation, we corrected the lag time estimation by subtracting the number of
512 dead cells $N_\mathrm{d}$ from the initial number $N(0) = A + B$. This gives a correction factor
513 $-\mu^{-1} \ln\left(\frac{N(0)}{N_\mathrm{d}}\right)$. For 5 h starvation at 45°C, about one third of the cells perish. Thus,
514 with growth rate 0.45/h at 45°C, this yields a correction factor of 0.9 h. In the main
515 text, all lag times are corrected for perished cells. Note that the bi-exponential fits
516 in Fig. 1, that include dynamics of both death and growth, are not used to extract
517 lag times.
518
519 *Time-lapse microscopy*
520 Microscopy was performed using agar pads in glass-bottom dishes. Agar pads
521 contained medium identical to the culture medium, $N^-C^-$ supplemented with 20
522 mM $NH_4Cl$, 20 mM Glycerol and 2 % low melting point agarose (Carl Roth,
523 Karlsruhe, Germany). Cells were diluted and pipetted on the prewarmed agar pad
524 and kept in the incubator. After the surface of the agar pad had dried, the agar pad
525 was flipped on the glass window of a prewarmed glass bottom dish. The glass
526 bottom dishes were sealed with parafilm to reduce evaporation.
527
528 Time-lapse microscopy was performed using a Nikon Ti-E microscope controlled
529 by NIS-Elements (Nikon, Tokyo, Japan). We used a phase contrast Plan Apo 100x
530 oil objective, with numerical aperture of 1.45 and a refractive index of 1.515
531 (Nikon, Tokyo, Japan) and a SCMOS camera (Zyla-5.5, Andor, Belfast, Northern
532 Ireland) with a binning of 1x1, a readout rate of 200 MHz and an exposure time of
533 200 ms. Conversion gain was set on 1/3 Dual gain and the spurious noise filter
534 was activated. The calibration from length units to pixels was defined as

535 0.07 µm/px. Measurements were performed with activated perfect focus system
536 and a PriorScan III drive stage. Temperature control was set by the Okolab Cage
537 Incubation System and confirmed with manual temperature measurements. Cell
538 growth was monitored for 24 hours with continuous acquisition of phase-contrast
539 and fluorescence images every 30 min at the desired temperature, e.g. 45°C.
540
541 *Live/dead stain*
542 Commercial BacLight®LIVE/DEAD (Thermo Fisher Scientific Inc., Waltham,
543 Massachusetts, USA) staining was used when cells were microscopically imaged,
544 according to manufacturing specifications.
545
546 *Heat shock protocol*
547 Heat shocks were performed by transferring batch cultures (5 ml culture volume
548 in a 20 mm x 150 mm borosilicate glass tube (Fisher Scientific, NH, USA)) from
549 one water bath to another (WSB-30, Witeg, Wertheim, Germany). Water baths
550 were pre-set and equilibrated at the desired temperatures.
551
552 *Survival quantification*
553 Survival in starvation was quantified by counting colony forming units (CFU).
554 Samples were diluted in carbon free $N^{-}C^{-}$ minimal medium and spread on LB
555 agar plates using Rattler Plating Beads (Zymo Research, Irvine, CA, USA) with a
556 target density of 200 colonies per plate. LB agar was supplemented with
557 25 µg/ml 2,3,5-triphenyltetrazolium chloride to stain colonies and increase
558 contrast for automated colony counting (Scan 1200, Interscience, Saint-Nom-la-
559 Bretèche, France). Staining or automation of counting had no significant effect on

viability measurements or accuracy, compared to unstained, manually counted samples (<1% systematic error). Petri dishes were 92 x 16 mm (Sarstedt, Nümbrecht, Germany) and agar plates were incubated for 12 hours at 37°C to ensure optimal colony size.

*Numerical analysis of the model*

The numerical solution in Fig. 3B was obtained by numerically integrating Eqs. (1-3) using the nonstiff differential equation solver *ode45* in Matlab (Mathworks, Natick, MA, USA). Initial conditions were $c_{\mathrm{met}}(0) = 0$ and $\phi_{\mathrm{MetA}}(0)$ ranging from $2 \cdot 10^{-5}$ to $2 \cdot 10^{-4}$. The parameters used in the calculations were $a_1 = 4.06\ \mathrm{M}^{-1}, a_2 = 3.1 \cdot 10^{-5}$, $a_3 = 148\ \mathrm{M}^{-2}$, $\chi_{\mathrm{MetA}} = 2.79 \cdot 10^{-3}$, $K_{\mathrm{M}} = 10^{-6}$ M, see Table S2.

The phase diagrams in Fig. S4 were calculated by solving Eq. (S12) using the *solve* function in Matlab (Mathworks, Natick, MA, USA). We shaded the regions according to the number of stable fixed-points at concentrations higher or equal to zero. One solution at $c^*_{\mathrm{met}} = 0$ (stable) was denoted 'non-growing region'. Two zeros, $c^{*,1}_{\mathrm{met}} = 0$ (unstable) and $c^{*,2}_{\mathrm{met}} > 0$ (stable) was denoted 'growth region'. Three zeros was denoted as the 'bistable region'. If methionine influx was included, Fig. S4E, one stable solution at $c^*_{\mathrm{met}} > 0$ means that cells can grow on external methionine. This region was shaded 'grey to white' to symbolize the growth rate dependence on the methionine influx. The parameters used in the calculations were $a_1 = 4.06\ \mathrm{M}^{-1}, a_2 = 3.1 \cdot 10^{-5}$, $a_3 = 148\ \mathrm{M}^{-2}$, $\chi_{\mathrm{MetA}} = 2.79 \cdot 10^{-3}$, $K_{\mathrm{M}} = 10^{-6}$ M, see Table S2.

585 *Statistical analysis*

586 Lag times with individual tests, e.g. methionine versus no methionine, were
587 performed in 2-3 biological repeats as mentioned in figure captions and are
588 reported with one standard deviation. Measurements that are quantitative tests,
589 e.g. influence of starvation time, were performed as single repeats, at multiple
590 different perturbation strength. Results of fits are reported with standard error.
591 Measurements of cell survival to antibiotic treatment were performed in
592 duplicates for each temperature. Survival measurements upon temperature shift
593 from 37, 40, 42 and 45 °C to 50°C were performed at least twice for wild-type and
594 MetA stabilized mutants.

595

596

597 **REFERENCES**

598 1. Yura, T. & Nakahigashi, K. Regulation of the heat-shock response. *Current*
599 *Opinion in Microbiology* **2**, 153–158 (1999).
600 2. Arsène, F., Tomoyasu, T. & Bukau, B. The heat shock response of Escherichia
601 coli. *International Journal of Food Microbiology* **55**, 3–9 (2000).
602 3. Richter, K., Haslbeck, M. & Buchner, J. The Heat Shock Response: Life on the
603 Verge of Death. *Molecular Cell* **40**, 253–266 (2010).
604 4. Bukau, B. Regulation of the Escherichia coli heat-shock response. *Molecular*
605 *Microbiology* **9**, 671–680 (1993).
606 5. Laskowska, E., Kuczyńska-Wiśnik, D., Skórko-Glonek, J. & Taylor, A.
607 Degradation by proteases Lon, Clp and HtrA, of Escherichia coli proteins
608 aggregated in vivo by heat shock; HtrA protease action in vivo and in vitro.
609 *Molecular Microbiology* **22**, 555–571 (1996).
610 6. Nonaka, G., Blankschien, M., Herman, C., Gross, C. A. & Rhodius, V. A. Regulon
611 and promoter analysis of the E. coli heat-shock factor, σ32, reveals a
612 multifaceted cellular response to heat stress. *Genes Dev.* **20**, 1776–1789
613 (2006).
614 7. Marcén, M., Ruiz, V., Serrano, M. J., Condón, S. & Mañas, P. Oxidative stress in E.
615 coli cells upon exposure to heat treatments. *International Journal of Food*
616 *Microbiology* **241**, 198–205 (2017).
617 8. Mackey, B. M. & Seymour, D. A. The Effect of Catalase on Recovery of Heat-
618 injured DNA-repair Mutants of Escherichia coli. *Microbiology,* **133**, 1601–1610
619 (1987).
620 9. Privalle, C. T. & Fridovich, I. Induction of superoxide dismutase in Escherichia
621 coli by heat shock. *PNAS* **84**, 2723–2726 (1987).

622 10. Marcén, M., Cebrián, G., Ruiz-Artiga, V., Condón, S. & Mañas, P. Protective effect
623 of glutathione on Escherichia coli cells upon lethal heat stress. *Food Research*
624 *International* **121**, 806–811 (2019).
625 11. Laman Trip, D. S. & Youk, H. Yeasts collectively extend the limits of habitable
626 temperatures by secreting glutathione. *Nature Microbiology* **5**, 943–954
627 (2020).
628 12. Ron, E. Z. & Davis, B. D. Growth Rate of Escherichia coli at Elevated
629 Temperatures: Limitation by Methionine. *J Bacteriol* **107**, 391–396 (1971).
630 13. Biran, D., Brot, N., Weissbach, H. & Ron, E. Z. Heat shock-dependent
631 transcriptional activation of the metA gene of Escherichia coli. *Journal of*
632 *bacteriology* **177**, 1374–1379 (1995).
633 14. Biran, D., Gur, E., Gollan, L. & Ron, E. Z. Control of methionine biosynthesis in
634 Escherichia coli by proteolysis. *Molecular Microbiology* **37**, 1436–1443 (2000).
635 15. Gur, E., Biran, D., Gazit, E. & Ron, E. Z. In vivo aggregation of a single enzyme
636 limits growth of Escherichia coli at elevated temperatures. *Molecular*
637 *Microbiology* **46**, 1391–1397 (2002).
638 16. Mordukhova, E. A., Lee, H.-S. & Pan, J.-G. Improved Thermostability and Acetic
639 Acid Tolerance of Escherichia coli via Directed Evolution of Homoserine o-
640 Succinyltransferase. *Appl Environ Microbiol* **74**, 7660–7668 (2008).
641 17. Ron, E. Z. Growth rate of Enterobacteriaceae at elevated temperatures:
642 limitation by methionine. *Journal of Bacteriology* **124**, 243–246 (1975).
643 18. Rotem, O., Biran, D. & Ron, E. Z. Methionine biosynthesis in Agrobacterium
644 tumefaciens: study of the first enzyme. *Research in Microbiology* **164**, 12–16
645 (2013).

646 19. Wyman, A., Shelton, E. & Paulus, H. Regulation of homoserine transacetylase
647 in whole cells of Bacillus polymyxa. *J. Biol. Chem.* **250**, 3904–3908 (1975).
648 20. Hwang, B.-J., Yeom, H.-J., Kim, Y. & Lee, H.-S. Corynebacterium glutamicum
649 Utilizes both Transsulfuration and Direct Sulfhydrylation Pathways for
650 Methionine Biosynthesis. *Journal of Bacteriology* **184**, 1277–1286 (2002).
651 21. Mordukhova, E. A., Kim, D. & Pan, J.-G. Stabilized homoserine o-
652 succinyltransferases (MetA) or L-methionine partially recovers the growth
653 defect in Escherichia coli lacking ATP-dependent proteases or the DnaK
654 chaperone. *BMC Microbiol* **13**, 179 (2013).
655 22. Gottesman, S. & Maurizi, M. R. Regulation by proteolysis: energy-dependent
656 proteases and their targets. *Microbiology and Molecular Biology Reviews* **56**,
657 592–621 (1992).
658 23. Mordukhova, E. A. & Pan, J.-G. Stabilization of Homoserine-O-
659 Succinyltransferase (MetA) Decreases the Frequency of Persisters in
660 Escherichia coli under Stressful Conditions. *PLOS ONE* **9**, e110504 (2014).
661 24. Balaban, N. Q., Merrin, J., Chait, R., Kowalik, L. & Leibler, S. Bacterial Persistence
662 as a Phenotypic Switch. *Science* **305**, 1622–1625 (2004).
663 25. Dill, K. A., Ghosh, K. & Schmit, J. D. Physical limits of cells and proteomes.
664 *Proceedings of the National Academy of Sciences* **108**, 17876–17882 (2011).
665 26. Leuenberger, P. *et al.* Cell-wide analysis of protein thermal unfolding reveals
666 determinants of thermostability. *Science* **355**, eaai7825 (2017).
667 27. Jung, I. L. & Kim, I. G. Polyamines and Glutamate Decarboxylase-based Acid
668 Resistance in *Escherichia coli*. *J. Biol. Chem.* **278**, 22846–22852 (2003).
669 28. Khan, A. U., Di Mascio, P., Medeiros, M. H. & Wilson, T. Spermine and
670 spermidine protection of plasmid DNA against single-strand breaks induced

671 by singlet oxygen. *Proceedings of the National Academy of Sciences* **89**, 11428–
672 11430 (1992).
673 29. Shah, P. & Swiatlo, E. A multifaceted role for polyamines in bacterial
674 pathogens. *Molecular Microbiology* **68**, 4–16 (2008).
675 30. Strogatz, S. H. *Nonlinear dynamics and chaos with student solutions manual:*
676 *With applications to physics, biology, chemistry, and engineering*. (CRC press,
677 2018).
678 31. Friedman, N., Cai, L. & Xie, X. S. Linking Stochastic Dynamics to Population
679 Distribution: An Analytical Framework of Gene Expression. *Phys. Rev. Lett.* **97**,
680 168302 (2006).
681 32. Taniguchi, Y. *et al.* Quantifying E. coli Proteome and Transcriptome with
682 Single-Molecule Sensitivity in Single Cells. *Science* **329**, 533–538 (2010).
683 33. Nierhaus, D. & Nierhaus, K. H. Identification of the Chloramphenicol-Binding
684 Protein in Escherichia coli Ribosomes by Partial Reconstitution. *PNAS* **70**,
685 2224–2228 (1973).
686 34. Davidson, J. F., Whyte, B., Bissinger, P. H. & Schiestl, R. H. Oxidative stress is
687 involved in heat-induced cell death in Saccharomyces cerevisiae. *PNAS* **93**,
688 5116–5121 (1996).
689 35. Davidson, J. F. & Schiestl, R. H. Cytotoxic and Genotoxic Consequences of Heat
690 Stress Are Dependent on the Presence of Oxygen in Saccharomyces cerevisiae.
691 *Journal of Bacteriology* **183**, 4580–4587 (2001).
692 36. Lushchak, V. I. & Bagnyukova, T. V. Temperature increase results in oxidative
693 stress in goldfish tissues. 1. Indices of oxidative stress. *Comparative*
694 *Biochemistry and Physiology Part C: Toxicology & Pharmacology* **143**, 30–35
695 (2006).

696 37. Lushchak, V. I. & Bagnyukova, T. V. Temperature increase results in oxidative
697 stress in goldfish tissues. 2. Antioxidant and associated enzymes. *Comparative*
698 *Biochemistry and Physiology Part C: Toxicology & Pharmacology* **143**, 36–41
699 (2006).
700 38. Murata, M. *et al.* Molecular Strategy for Survival at a Critical High Temperature
701 in Eschierichia coli. *PLOS ONE* **6**, e20063 (2011).
702 39. Mirzaei, H. & Regnier, F. Protein:protein aggregation induced by protein
703 oxidation. *Journal of Chromatography B* **873**, 8–14 (2008).
704 40. Lévy, E. *et al.* Causative Links between Protein Aggregation and Oxidative
705 Stress: A Review. *International Journal of Molecular Sciences* **20**, 3896 (2019).
706 41. Davies, K. J. A. & Lin, S. W. Degradation of oxidatively denatured proteins in
707 Escherichia coli. *Free Radical Biology and Medicine* **5**, 215–223 (1988).
708 42. Pacifici, R. E. & Davies, K. J. A. Protein degradation as an index of oxidative
709 stress. in *Methods in Enzymology* vol. 186 485–502 (Academic Press, 1990).
710 43. Oliver, J. D. Recent findings on the viable but nonculturable state in pathogenic
711 bacteria. *FEMS Microbiol Rev* **34**, 415–425 (2010).
712 44. Xu, H.-S. *et al.* Survival and viability of nonculturableEscherichia coli andVibrio
713 cholerae in the estuarine and marine environment. *Microb Ecol* **8**, 313–323
714 (1982).
715 45. Oliver, J. D. The viable but nonculturable state in bacteria. *J. Microbiol.* **43 Spec**
716 **No**, 93–100 (2005).
717 46. Balaban, N. Q. *et al.* Definitions and guidelines for research on antibiotic
718 persistence. *Nature Reviews Microbiology* **17**, 441–448 (2019).

719 47. Li, L., Mendis, N., Trigui, H., Oliver, J. D. & Faucher, S. P. The importance of the
720 viable but non-culturable state in human bacterial pathogens. *Front. Microbiol.*
721 **5**, (2014).
722 48. Zhao, X., Zhong, J., Wei, C., Lin, C.-W. & Ding, T. Current Perspectives on Viable
723 but Non-culturable State in Foodborne Pathogens. *Front. Microbiol.* **8**, (2017).
724 49. Pinto, D., Santos, M. A. & Chambel, L. Thirty years of viable but nonculturable
725 state research: Unsolved molecular mechanisms. *Critical Reviews in*
726 *Microbiology* **41**, 61–76 (2015).
727 50. Harms, A., Maisonneuve, E. & Gerdes, K. Mechanisms of bacterial persistence
728 during stress and antibiotic exposure. *Science* **354**, aaf4268 (2016).
729 51. Potrykus, K. & Cashel, M. (p)ppGpp: Still Magical? *Annual Review of*
730 *Microbiology* **62**, 35–51 (2008).
731 52. Lemke, J. J. *et al.* Direct regulation of Escherichia coli ribosomal protein
732 promoters by the transcription factors ppGpp and DksA. *PNAS* **108**, 5712–
733 5717 (2011).
734 53. Dalebroux, Z. D. & Swanson, M. S. ppGpp: magic beyond RNA polymerase. *Nat*
735 *Rev Microbiol* **10**, 203–212 (2012).
736 54. Schreiber, G., Ron, E. Z. & Glaser, G. ppGpp-mediated regulation of DNA
737 replication and cell division in Escherichia coli. *Current Microbiology* **30**, 27–
738 32 (1995).
739 55. Wang, J. D., Sanders, G. M. & Grossman, A. D. Nutritional Control of Elongation
740 of DNA Replication by (p)ppGpp. *Cell* **128**, 865–875 (2007).
741 56. Price-Carter, M., Fazzio, T. G., Vallbona, E. I. & Roth, J. R. Polyphosphate Kinase
742 Protects Salmonella enterica from Weak Organic Acid Stress. *Journal of*
743 *Bacteriology* **187**, 3088–3099 (2005).

744 57. Gardner, A., West, S. A. & Griffin, A. S. Is Bacterial Persistence a Social Trait?
745 *PLoS ONE* **2**, e752 (2007).
746 58. Veening, J.-W., Smits, W. K. & Kuipers, O. P. Bistability, Epigenetics, and Bet-
747 Hedging in Bacteria. *Annual Review of Microbiology* **62**, 193–210 (2008).
748 59. Verstraeten, N. *et al.* Obg and Membrane Depolarization Are Part of a Microbial
749 Bet-Hedging Strategy that Leads to Antibiotic Tolerance. *Molecular Cell* **59**, 9–
750 21 (2015).
751 60. Soupene, E. *et al.* Physiological Studies of Escherichia coli Strain MG1655:
752 Growth Defects and Apparent Cross-Regulation of Gene Expression. *J Bacteriol*
753 **185**, 5611–5626 (2003).
754 61. Csonka, L. N., Ikeda, T. P., Fletcher, S. A. & Kustu, S. The accumulation of
755 glutamate is necessary for optimal growth of Salmonella typhimurium in
756 media of high osmolality but not induction of the proU operon. *Journal of*
757 *Bacteriology* **176**, 6324–6333 (1994).
758
759